

Article

Analytical Description of an Axisymmetric Supercavitation Bubble in a Viscous Flow

Lotan Arad Ludar and Alon Gany * 

Faculty of Aerospace Engineering, Technion—Israel Institute of Technology, Haifa 32000, Israel

* Correspondence: gany@tx.technion.ac.il

Abstract: One of the basic elements which characterizes flow regimes, is viscosity. This element has typically been neglected in research on supercavitational flows, describing and predicting supercavitation bubbles geometry and formation using non-viscous potential flows. Arguing that the viscosity effect is much smaller than the inertial effect at high flow speeds, the viscosity has been ignored and the only parameter for modeling the flow has been the cavitation number. However, for some situations and conditions, the viscosity was found to be significant and crucial for the bubble geometry and formation, especially at the supercavitation bubble detachment point, hence some investigations based on numerical calculations have taken viscosity into account. This paper presents an analytical model of an axisymmetric supercavitation bubble in a viscous flow according to Serebryakov annular model for calculation of axisymmetric cavity flows. Viscosity effect on the bubble geometry is suggested, and an analysis for validation and examination is presented as well. The results show the change of the bubble formation from past models due to the viscosity, and offer a more accurate description of the bubble geometry close to the detachment point. Moreover, the slenderness parameter is calculated and presented for supercavitation bubbles in a viscous flow together with its dependency on Reynolds number and the cavitation number. The analysis reveals that the slenderness parameter increases with increasing both the cavitation number and Reynolds number, where the latter has a substantial effect.

Keywords: supercavitation; bubble geometry; viscous flow; viscosity effect; slenderness parameter; cavitation number



Citation: Arad Ludar, L.; Gany, A. Analytical Description of an Axisymmetric Supercavitation Bubble in a Viscous Flow. *J. Mar. Sci. Eng.* **2022**, *10*, 2029. <https://doi.org/10.3390/jmse10122029>

Academic Editors: Simone Mancini and Momchil Terziev

Received: 10 November 2022

Accepted: 11 December 2022

Published: 19 December 2022

Publisher's Note: MDPI stays neutral with regard to jurisdictional claims in published maps and institutional affiliations.



Copyright: © 2022 by the authors. Licensee MDPI, Basel, Switzerland. This article is an open access article distributed under the terms and conditions of the Creative Commons Attribution (CC BY) license (<https://creativecommons.org/licenses/by/4.0/>).

1. Introduction

Supercavitation bubbles have been studied for decades because of their significance for the design of supercavitation vehicles and applications. In order to improve performance of high-speed underwater vehicles and save energy by drag reduction through minimizing the friction in water, many investigations have been conducted to develop a theory to this unique phenomenon [1,2]. In most cases, analyses for describing and predicting supercavitation bubbles geometry and formation used non-viscous potential flows, arguing that viscosity effect is much smaller than inertial effects. Much effort has been made to establish theoretical analyses of supercavitation flow based on those assumptions. Proposing methods of calculation and presenting relations between the bubble dimensions and the flow conditions, most studies have particularly examined axisymmetric supercavitation bubbles [3–6]. Tulin [7] presented a two-dimensional slender body theory for modeling supercavitating flows, and Gilbarg [8] showed a solution of non-thin wedges. Semenenko [9] proposed the basic physical properties and computational methods for artificial cavitation (ventilation) flows. Vasin [10–13] explored the supercavitation flow field under subsonic, transonic, and supersonic conditions based on the slender body theory, and analyzed the cavitation state and stress characteristics under corresponding conditions. In 1969, Logvinovich [14] proposed the principle of independent expansion of cavitation sections. Vasin [15] and Serebryakov [16] derived the section development equation based on this

principle. Fu et al. [17] studied the supercavitation resistance characteristics of a rotating body based on the Kubota cavitation model. Yi et al. [18] studied the change in the drag coefficient of a supercavitating vehicle at different speeds and explored the relationship between the drag coefficient and cavitator diameter. Other studies have analyzed the wall effect in channels on the bubble dimensions as well as the values of the cavitation number of fully developed cavitation bubbles [19]. Some experimental works showed the development of axially symmetric supercavities in bounded and unbounded flows and examined the bubble characteristics with relation to natural and artificial supercavitation [20,21]. Karn [22] revealed the effect of internal flow physics on the characteristics observed during supercavity formation and closed mode transitions. Ahn [20] analyzed the general characteristics of supercavitation and experimentally observed the size of supercavitation. The role of the cavitator in determining the bubble shape and size has been found to be very effective in the supercavitation bubble development and existence. This has been examined analytically for 2D flows [23], numerically for 3D flows for more accurate results and for specific geometries [24], and experimentally [25,26]. Some estimations and predictions have been done mainly for unbounded bubbles [14,15,21,27–30]. Other experimental investigations have described the bubbles formed on different bodies, examining the gravitation effect, the closing modes, the separation point, and more. Many of them are summarized by Franc and Michel [31]. Typically, in the high-speed supercavitational flows, the only parameter used to model the flows was the cavitation number, neglecting viscosity effect. Nevertheless, for some situations and conditions, the viscosity was found to be significant and even crucial for the bubble geometry and formation, especially at the supercavitation bubble detachment point. Hence, some research based on numerical calculations, have taken the viscosity into account [32]. Yet, no analytical model has been established.

This paper presents an analytical model of an axisymmetric supercavitation bubble in a viscous flow following Serebryakov [4,33] annular model for calculation of axisymmetric cavity flows. The viscosity effect of the bubble geometry is suggested, together with an analysis examining the resulting dimensions.

2. Problem Description

We have considered an axisymmetric supercavitation bubble developing along a cylindrical object in a uniform flow of liquid. A slender cylindrical body has been examined. When the pressure decreases below the equilibrium vapor pressure of the liquid, the liquid starts to evaporate, developing a supercavitation bubble over the body. As the flow velocity increases, the pressure decreases, the reduced pressure zone broadens, and the bubble grows and can envelope the entire body (see Figure 1). In a steady flow, the bubble shape and dimensions become practically constant, being determined by the flow conditions and fluid characteristics as well as by the geometry of the cavitator, the body, and the surrounding. The viscosity is one of the fluid characteristics that determines the flow regime, the phase transition, and finally the supercavitation bubble development, shape, and dimensions.

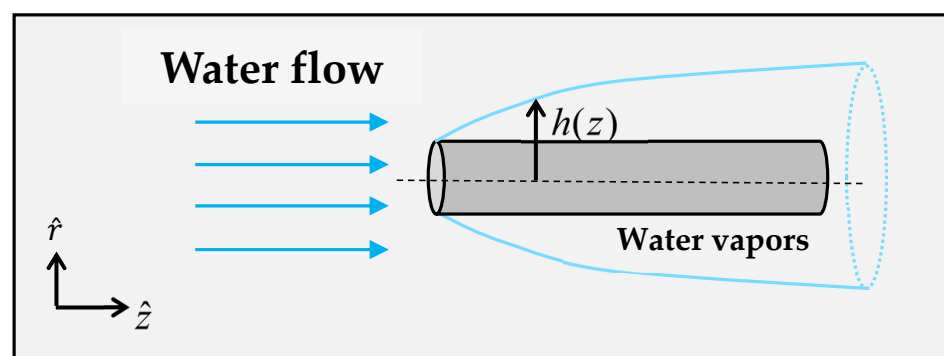


Figure 1. A scheme of the physical problem.

3. Analytical Analyses

3.1. Dimension Approximation

We have considered a thin film axisymmetric supercavitation bubble in a steady flow with velocity U_∞ . z and r are the axial and the radial coordinates, respectively, whereas the location in the volume will be signed as $z\hat{z} + r\hat{r}$. $h(z)$ is the bubble width. H is the characteristic dimension of the bubble, whereas its characteristic length is L . From the conservation of mass in potential flow (Equation (1)), the radial velocity is of the order $U_\infty \frac{H}{L}$ and it is much smaller than the axial velocity. Equation (1) refers to the bubble vapor medium, having constant pressure, temperature, and density.

$$\frac{1}{r} \frac{\partial(ru_r)}{\partial r} + \frac{\partial u_z}{\partial z} = 0 \tag{1}$$

For axisymmetric steady viscous flow, Navier–Stokes equation narrows to:

$$\begin{aligned} \rho \left(u_r \frac{\partial u_r}{\partial r} + u_z \frac{\partial u_r}{\partial z} \right) &= -\frac{\partial P}{\partial r} + \rho g_r + \mu \left[\frac{1}{r} \frac{\partial}{\partial r} \left(r \frac{\partial u_r}{\partial r} \right) - \frac{u_r}{r^2} + \frac{\partial^2 u_r}{\partial z^2} \right] \\ \rho \left(u_r \frac{\partial u_z}{\partial r} + u_z \frac{\partial u_z}{\partial z} \right) &= -\frac{\partial P}{\partial z} + \mu \left[\frac{1}{r} \frac{\partial}{\partial r} \left(r \frac{\partial u_z}{\partial r} \right) + \frac{\partial^2 u_z}{\partial z^2} \right] \end{aligned} \tag{2}$$

Neglecting small orders, the pressure gradient in both radial and axial directions and the body forces in the radial direction can be approximated:

$$\begin{aligned} \frac{\partial P}{\partial r} - \rho g_r &\sim -\rho U_\infty^2 \frac{H}{L^2} + \mu \frac{U_\infty}{LH} \\ \frac{\partial P}{\partial z} &\sim -\rho \frac{U_\infty^2}{L} + \mu \frac{U_\infty}{H^2} \end{aligned} \tag{3}$$

From the axial direction the inertial forces versus the viscosity forces can be examined (see Equation (4)). For sufficiently large velocity, where the bubble length is much larger than its width, the viscosity can be neglected, and the pressure gradient in the axial direction will change only due to the dynamic pressure as $\sim \rho U_\infty^2$.

$$\frac{\rho U_\infty^2}{L} / \mu \frac{\rho U_\infty}{H^2} = \frac{\rho U_\infty L}{\mu} \left(\frac{H}{L} \right)^2 = \text{Re} \left(\frac{H}{L} \right)^2 \tag{4}$$

In the radial direction, the inertial effect could also be neglected for the case of small viscosity (see Equation (5)), and the pressure in the radial direction will change only due to body forces, whereas for small bubble width this effect will be negligible as well.

$$P \sim \rho U_\infty^2 \left(\frac{H^2}{L^2} \right) \tag{5}$$

For small velocities, when there is a large bubble expansion in the radial dimension and a small extension of the bubble length, the viscosity will have a greater effect and the pressure gradient in the radial direction will dominate (see Equation (6)) as opposed to the axial changes of the pressure that will be negligible (see Equation (7)).

$$\frac{\partial P}{\partial r} \sim \frac{\mu U_\infty}{HL} \tag{6}$$

$$\frac{\partial P}{\partial z} \sim \frac{\mu U_\infty}{H^2} \tag{7}$$

3.2. Supercavitation Bubble Geometry in a Viscous Flow

To describe a supercavitation bubble geometry in a viscous flow using a slender body theory, and assuming that the changes along the symmetry axis are much smaller than the radial changes, Equation (1) narrows to:

$$\frac{1}{r} \frac{\partial(ru_r)}{\partial r} \approx 0 \tag{8}$$

And so:

$$ru_r = C(z) \tag{9}$$

where $C(z)$ is determined from the boundary conditions of the bubble surface, where the radial velocity is:

$$\frac{u_r(R, z)}{U_\infty} = \frac{dR}{dz} \tag{10}$$

Deducing the radial velocity (see Equation (11)) and substituting to the Navier–Stokes equations in cylindrical coordinates,

$$u_r = \frac{1}{2} \frac{U_\infty}{r} \frac{dR^2}{dz} \tag{11}$$

we get the equation:

$$\frac{1}{\frac{1}{2}\rho U_\infty^2} \frac{\partial P}{\partial r} = R^2 \left(\frac{dR}{dz} \right)^2 \frac{2}{r^3} - \frac{d^2 R^2}{dz^2} \frac{1}{r} + \frac{\mu}{U_\infty} \frac{d^3 R^2}{dz^3} \tag{12}$$

The cavitation number is defined as follows:

$$\sigma_c = \frac{p_\infty - p_c}{\frac{1}{2}\rho U_\infty^2} \tag{13}$$

Integrating Equation (13) between the radius R of the cavity where the pressure equals the cavity pressure P_c , and the radius $\psi(z)$ far away from the cavity representing the pressure at infinity, we get the relation:

$$\sigma_c = R^2 \left(\frac{\partial R}{\partial z} \right)^2 \left(\frac{1}{R^2} - \frac{1}{\psi^2} \right) + \left[\frac{\mu}{\rho U_\infty} \frac{\partial^3 (R^2)}{\partial z^3} - \frac{\partial^2 (R^2)}{\partial z^2} \right] \ln \left(\frac{\psi}{R} \right) \tag{14}$$

where ψ is far from the bubble, where the flow is no longer disturbed by the cavitation process; so, by assuming $\psi \gg R$, the expression narrows to:

$$\frac{\sigma_c}{\ln \left(\frac{\psi}{R} \right)} \approx \frac{\mu}{\rho U_\infty} \frac{\partial^3 (R^2)}{\partial z^3} - \frac{\partial^2 (R^2)}{\partial z^2} \tag{15}$$

To solve the differential equation, we will first define:

$$f(z) = R^2(z) \tag{16}$$

and integrate twice Equation (15), so the relation comes down to:

$$\frac{\mu}{\rho U_\infty} f' - f = \frac{\sigma_c}{2 \ln \left(\frac{\psi}{R} \right)} z^2 + C_1 z + C_2 \tag{17}$$

where C_1, C_2 are constants depending on the boundary conditions.

First we will solve the homogenous equation of (17) and derive:

$$f = C_3 e^{\frac{\rho U_\infty}{\mu} z} \tag{18}$$

Suggesting a solution to the inhomogeneous equation and substituting its first derivative:

$$f = C_3(z) e^{\frac{\rho U_\infty}{\mu} z}, f' = C_3'(z) e^{\frac{\rho U_\infty}{\mu} z} + C_3(z) \frac{\rho U_\infty}{\mu} e^{\frac{\rho U_\infty}{\mu} z} \tag{19}$$

we get:

$$C_3'(z) = \frac{\rho U_\infty}{\mu} \left(\frac{\sigma_c}{2 \ln\left(\frac{\psi}{R}\right)} z^2 + C_1 z + C_2 \right) e^{-\frac{\rho U_\infty}{\mu} z} \tag{20}$$

$$C_3(z) = -e^{-\frac{\rho U_\infty}{\mu} z} \left(\frac{\sigma_c}{2 \ln\left(\frac{\psi}{R}\right)} z^2 + C_1 z + C_2 + \left(\frac{\sigma_c}{\ln\left(\frac{\psi}{R}\right)} z + C_1 \right) \frac{\mu}{\rho U_\infty} + \frac{\sigma_c}{\ln\left(\frac{\psi}{R}\right)} \left(\frac{\mu}{\rho U_\infty} \right)^2 \right) \tag{21}$$

The solution of the equation yields the radius change along the symmetry axis:

$$R^2 = -\frac{\sigma_c}{2 \ln\left(\frac{\psi}{R}\right)} z^2 - C_1 z - C_2 - \left(\frac{\sigma_c}{\ln\left(\frac{\psi}{R}\right)} z + C_1 \right) \frac{\mu}{\rho U_\infty} - \frac{\sigma_c}{\ln\left(\frac{\psi}{R}\right)} \left(\frac{\mu}{\rho U_\infty} \right)^2 + C_3 e^{\frac{\rho U_\infty}{\mu} z} \tag{22}$$

To prevent divergence for small values of viscosity or high speeds characterizing super-cavitational flows, as well as for locations far from the front edge, we argue $C_3 \approx 0$, hence:

$$R^2 = -\frac{\sigma_c}{2 \ln\left(\frac{\psi}{R}\right)} z^2 - C_1 z - C_2 - \left(\frac{\sigma_c}{\ln\left(\frac{\psi}{R}\right)} z + C_1 \right) \frac{\mu}{\rho U_\infty} - \frac{\sigma_c}{\ln\left(\frac{\psi}{R}\right)} \left(\frac{\mu}{\rho U_\infty} \right)^2 \tag{23}$$

We will define dimensionless numbers, which describes a geometrical relation:

$$\Delta \triangleq \ln\left(\frac{\Psi}{R}\right) \tag{24}$$

and also define Reynolds number characterizing the flow:

$$Re = \frac{\rho U_\infty l_c}{\mu} \tag{25}$$

The geometrical relation mentioned in Equation (24) characterizes the inertial properties of the liquid annular layer and plays the role of an added mass. For small values of the slenderness parameter measured by the ratio of the maximum diameter of the cavity d_c to its length l_c :

$$\delta = \frac{d_c}{l_c} \tag{26}$$

the parameter Δ can be considered as constant and dependent only upon the cavity slenderness δ as was also applied by Serebryakov [4,33].

The solution (Equation (23)) of the equation narrows down to:

$$R^2 = -\frac{\sigma_c}{2\Delta} z^2 - C_1 z - C_2 - \left(\frac{\sigma_c}{\Delta} z + C_1 \right) \frac{l_c}{Re} - \frac{\sigma_c}{\Delta} \frac{l_c^2}{Re^2} \tag{27}$$

where:

$$\begin{aligned} C_1 &= \frac{-R_{edge}^2 + 2R_{cavitator}R_{edge}}{l_c} - \frac{\sigma_c}{\Delta} l_c \left(\frac{1}{Re} + \frac{1}{2} \right) \\ C_2 &= \frac{R_{edge}^2 - 2R_{cavitator}R_{edge}}{Re} + \frac{\sigma_c}{2\Delta Re} l_c^2 - R_{cavitator}^2 \end{aligned} \tag{28}$$

where l_c is the bubble length.

Substituting Equation (28) into Equation (27), the bubble radius will be:

$$R^2 = -\frac{\sigma_c}{2\Delta} z^2 - \left(\frac{-R_{edge}^2 + 2R_{cavitator}R_{edge}}{l_c} - \frac{\sigma_c}{2\Delta} l_c \right) z + R_{cavitator}^2 \tag{29}$$

For a closed bubble, where $R_{edge} = R_{cavitator}$:

$$R^2 = -\frac{\sigma_c}{2\Delta} z^2 - \left(\frac{R_{cavitator}^2}{l_c} - \frac{\sigma_c}{2\Delta} l_c \right) z + R_{cavitator}^2 \tag{30}$$

For homogeneous boundary conditions with defining $R_{cavitator} = 0$, Equation (30) narrows to:

$$R^2 = -\frac{\sigma_c}{2\Delta} z^2 + \frac{\sigma_c}{2\Delta} l_c z \tag{31}$$

We get Serebryakov [33] model of an elliptic bubble:

$$\frac{R^2}{\frac{\sigma_c}{2\Delta} \frac{l_c^2}{4}} + \frac{\left(z - \frac{l_c}{2} \right)^2}{\frac{l_c^2}{4}} = 1 \tag{32}$$

This derivation was made for potential non-viscous flow from Euler equation. The components which are dependent on the viscosity, were naturally eliminated, and the radius describing the bubble geometry along the body is independent of Reynold number and thus independent of the viscosity.

For large values of viscosity or short bubble length, as well as for locations close to the front edge where the initial cavitation starts, the last component of Equation (22) should not be ignored and the exponent can be expressed with a Taylor expansion for small argument tends to zero (see Equation (33)).

$$R^2 = -\frac{\sigma_c}{2\ln\left(\frac{\psi}{R}\right)} z^2 - C_1 z - C_2 - \left(\frac{\sigma_c}{\ln\left(\frac{\psi}{R}\right)} z + C_1 \right) \frac{\mu}{\rho U_\infty} - \dots \tag{33}$$

$$\dots - \frac{\sigma_c}{\ln\left(\frac{\psi}{R}\right)} \left(\frac{\mu}{\rho U_\infty} \right)^2 + C_3 \left(1 + \text{Re} \frac{z}{l_c} + \frac{1}{2} \left(\text{Re} \frac{z}{l_c} \right)^2 + \frac{1}{6} \left(\text{Re} \frac{z}{l_c} \right)^3 + O \left(\text{Re} \frac{z}{l_c} \right)^4 \right)$$

Equation (33) with the defined numbers of Equations (24) and (25):

$$R^2 = -\frac{\sigma_c}{2\Delta} z^2 - C_1 z - C_2 - \left(\frac{\sigma_c}{\Delta} z + C_1 \right) \frac{l_c}{\text{Re}} - \frac{\sigma_c}{\Delta} \left(\frac{l_c}{\text{Re}} \right)^2 + \dots \tag{34}$$

$$\dots + C_3 \left(1 + \text{Re} \frac{z}{l_c} + \frac{1}{2} \left(\text{Re} \frac{z}{l_c} \right)^2 + \frac{1}{6} \left(\text{Re} \frac{z}{l_c} \right)^3 + O \left(\text{Re} \frac{z}{l_c} \right)^4 \right)$$

Substituting boundary conditions (Equation (35)) into Equation (34) we will find the constants C_1, C_2, C_3 .

$$\begin{aligned} R(0) &= 0 \\ R(l_c) &= 0 \\ f'(0) &= \frac{\partial R^2}{\partial z} = 2R(0) \frac{\partial R}{\partial z} \Big|_{z=0} = 0 \end{aligned} \tag{35}$$

The boundary conditions describe a closed bubble where the radius of the bubble starts at the body's surface.

The three constants C_1, C_2, C_3 :

$$\begin{aligned} C_1 &= \frac{\frac{\sigma_c l_c}{\Delta Re}}{1 + \frac{1}{3} Re + O(Re)^2} \left(1 + \frac{1}{2} Re + \frac{1}{6} Re^2 + O(Re)^3 \right) - \frac{\sigma_c}{\Delta Re} l_c - \frac{\sigma_c}{2\Delta} l_c \\ C_2 &= 0 \\ C_3 &= \frac{\frac{\sigma_c}{\Delta Re} l_c^2}{Re + \frac{1}{3} Re^2 + O(Re)^3} \end{aligned} \tag{36}$$

Substituting them (Equation (36)) into the radius expression (Equation (34)), we get:

$$\begin{aligned} R^2 &= -\frac{\sigma_c}{2\Delta} z^2 - \left(\frac{\frac{\sigma_c}{\Delta Re} l_c}{1 + \frac{1}{3} Re + O(Re)^2} \left(1 + \frac{1}{2} Re + \frac{1}{6} Re^2 + O(Re)^3 \right) - \frac{\sigma_c}{\Delta Re} l_c - \frac{\sigma_c}{2\Delta} l_c \right) z - \dots \\ &\dots - \frac{\sigma_c}{\Delta} \frac{l_c}{Re} z - \frac{\frac{\sigma_c}{\Delta} \left(\frac{l_c}{Re} \right)^2}{1 + \frac{1}{3} Re + O(Re)^2} \left(1 + \frac{1}{2} Re + \frac{1}{6} Re^2 + O(Re)^3 \right) + \frac{\sigma_c}{\Delta} \left(\frac{l_c}{Re} \right)^2 + \frac{\sigma_c}{2\Delta Re} l_c^2 - \dots \\ &\dots - \frac{\sigma_c}{\Delta} \left(\frac{l_c}{Re} \right)^2 + \frac{\frac{\sigma_c}{\Delta Re} l_c^2}{Re + \frac{1}{3} Re^2 + O(Re)^3} \left(1 + Re \frac{z}{l_c} + \frac{1}{2} \left(Re \frac{z}{l_c} \right)^2 + \frac{1}{6} \left(Re \frac{z}{l_c} \right)^3 + O \left(Re \frac{z}{l_c} \right)^4 \right) \end{aligned} \tag{37}$$

After combining and narrowing down the expression, also neglecting high order terms:

$$R^2 = -\frac{\sigma_c}{2\Delta} z^2 + \frac{\sigma_c}{2\Delta Re^2} l_c z + \frac{\frac{\sigma_c}{2\Delta}}{1 + \frac{1}{3} Re + O(Re)^2} \left(z^2 + \frac{1}{3} \left(\frac{Re}{l_c} \right) z^3 + O(z^4) \right) \tag{38}$$

$$R^2 \approx \left(\frac{\sigma_c}{2\Delta} \left(1 - \frac{1}{3} Re + O(Re)^2 \right) - \frac{\sigma_c}{2\Delta} \right) z^2 + \frac{\sigma_c}{2\Delta Re^2} l_c z + \frac{\sigma_c}{2\Delta} \frac{1}{3} \left(\frac{Re}{l_c} \right) \left(1 - \frac{1}{3} Re + O(Re)^2 \right) z^3 \tag{39}$$

$$R^2 \approx -\frac{\sigma_c}{6\Delta} Re z^2 + \frac{\sigma_c}{2\Delta Re^2} l_c z + \frac{\sigma_c}{2\Delta} \frac{1}{3} \left(\frac{Re}{l_c} \right) z^3 \tag{40}$$

Equation (40) can also be written as:

$$\frac{R^2}{\frac{3\sigma_c}{8\Delta} \frac{l_c^2}{Re}} + \frac{\left(z - \frac{3}{2} \frac{l_c}{Re} \right)^2}{\left(\frac{3}{2} \frac{l_c}{Re} \right)^2} = 1 + \left(\frac{2}{3} Re \right)^2 \left(\frac{z}{l_c} \right)^3 \tag{41}$$

Neglecting small terms:

$$\left(\frac{2}{3} Re \right)^2 \left(\frac{z}{l_c} \right)^3 \rightarrow 0 \tag{42}$$

we gain the elliptic relation:

$$\frac{R^2}{\frac{\sigma_c}{2\Delta} \frac{l_c^2}{4} \left(\frac{3}{Re} \right)} + \frac{\left(z - \left(\frac{3}{Re} \right) \frac{l_c}{2} \right)^2}{\left(\frac{3}{Re} \right)^2 \frac{l_c^2}{4}} = 1 \tag{43}$$

4. Results and Discussions

The addition of the viscosity stresses to the cavitation flow modeling revealed a similar relation of the geometrical shape of the supercavitation bubble in a non-viscous flow.

Equation (43), for a bubble in a viscous flow, describes an elliptic relation similarly to the relation presented in Equation (30), which describes a bubble in a non-viscous flow. The viscosity, which is dominant for small values of bubble length and close to the front edge, causes an expansion in the bubble dimensions in both radial and axial directions, as well as a change in the location of the bubble center. Figure 2 presents the change in the ellipse that describes the bubble, but the real change will be at the front edge, where the assumptions are valid.

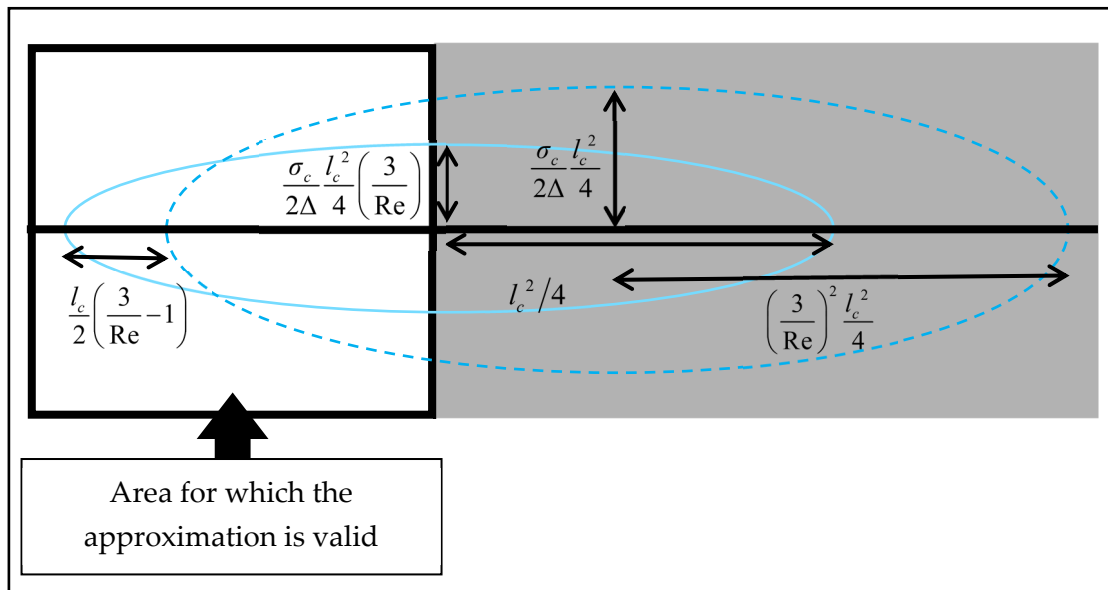


Figure 2. A scheme of the bubble dimensions change.

The cavity slenderness parameter mentioned in Equation (26) can be the best evaluation for the viscous effect of the supercavitation bubble dimensions.

The denominator of the first component of Equation (43) is related to the denominator of the second component of the equation, which describes the expansion—extension of the bubble, expresses the slenderness parameter. The ratio between the denominator of the first component of Equation (32) and the denominator of the second component of the equation differs from the first ratio by $3/Re$, differing from the bubble dimensions in a viscous flow as compared to a non-viscous flow.

The cavity slenderness is given by:

$$\delta = \sqrt{\frac{\sigma_c}{2\Delta} \frac{3}{Re}} \tag{44}$$

Substituting Equation (44) into Equation (24) we get:

$$\Delta = \ln\left(\frac{2\Psi}{d_c}\right) = \ln\left(\frac{2\Psi}{\delta l_c}\right) = \ln\left(\frac{2\Psi}{l_c} \sqrt{\frac{3}{Re} \frac{\sigma_c}{2\Delta}}\right) \tag{45}$$

Dividing the logarithm in Equation (45) to three components:

$$\Delta = \frac{1}{2} \ln\left(\frac{3}{Re} \frac{1}{\sigma_c}\right) + \frac{1}{2} \ln \Delta + \ln\left(\frac{2\Psi}{l_c} \sqrt{2}\right) \tag{46}$$

the second component in the right hand side of Equation (46) can be neglected with respect to Δ , the third component is almost constant, and the first component which is significant to supercavitation flows for small cavitation numbers as well as for small Reynolds numbers for viscous flows, obtains the asymptotic relation:

$$2\Delta \approx \ln\left(\frac{3}{Re\sigma_c}\right) \tag{47}$$

Substituting into the slenderness parameter (Equation (44)), we obtain:

$$\delta = \sqrt{\frac{Re\sigma_c}{3} \frac{1}{\ln\left(\frac{3}{Re\sigma_c}\right)}} \tag{48}$$

This relation is similar to Garbedian [34] relation and the asymptotic relation of Serebryakov [33] for non-viscous flow (see Equation (49)), without Reynolds number effect, which expresses the viscosity influence on the flow:

$$\delta = \sqrt{\sigma_c \frac{1}{\ln\left(\frac{1}{\sigma_c}\right)}} \tag{49}$$

Figure 3 shows the change in the slenderness parameter with the change of the cavitation number for different Reynolds numbers. The slenderness parameter gets bigger for smaller Reynolds number, for every cavitation number, whereas the viscosity has a smaller effect, and so the bubble extends. This was expected, as evaluated by dimension approximation in Section 3.1, which showed expansion in the radial direction together with a small effect of viscosity (small Reynolds numbers).

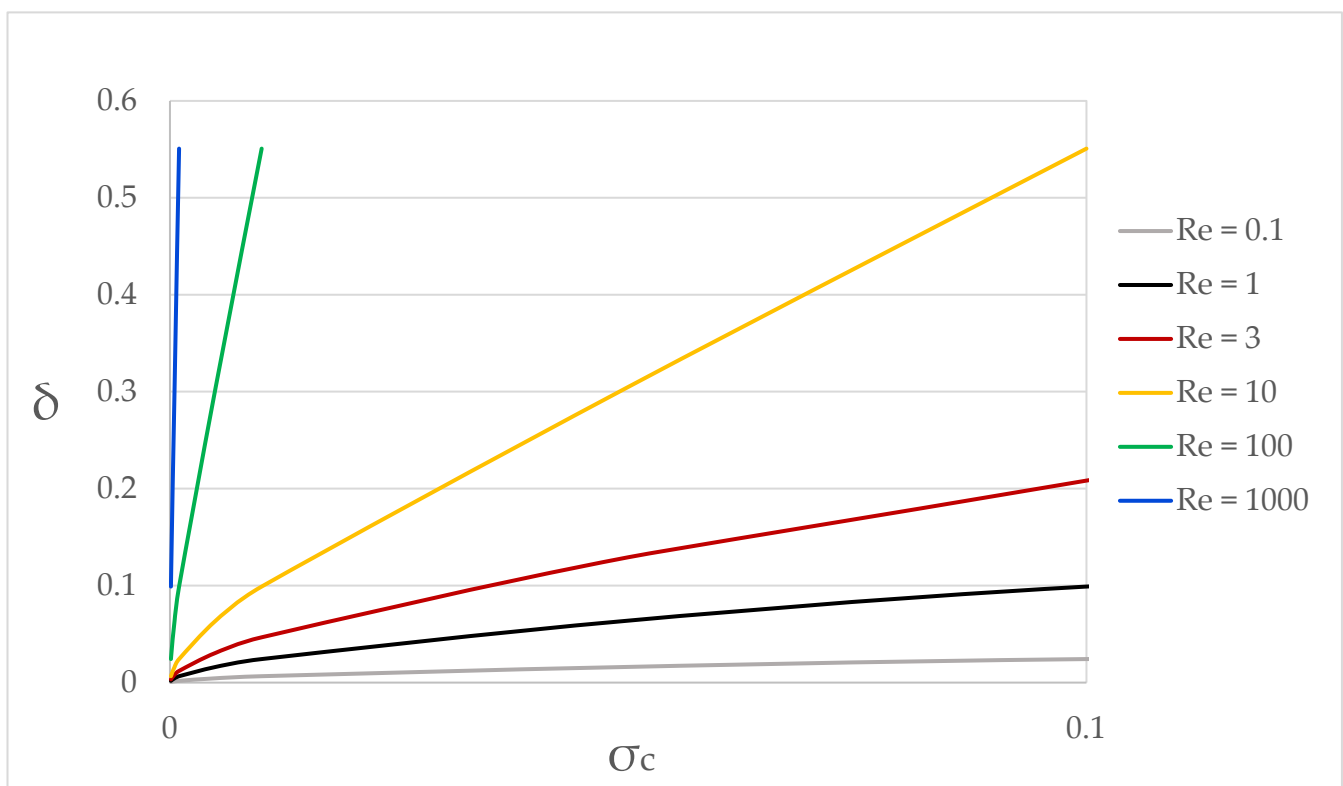


Figure 3. The slenderness parameter vs. the cavitation number for different Reynolds numbers.

5. Conclusions

The viscosity, which is one of the basic elements that characterizes flow regimes and has usually been neglected in the research of supercavitational flows, must be taken into account in the modeling of supercavitation bubbles. For some cases, especially at the supercavitation bubble detachment point, the viscosity has a significant and even crucial effect in determining accurately the bubble geometry and formation. The bubble geometry that was described as an ellipsoid in a non-viscous potential flow by Serebryakov (1972) [33], was found in this work to have an elliptic shape in a viscous flow as well. The viscosity was found to be dominant for small values of bubble length and close to the front edge, causing expansion of the bubble dimensions in both radial and axial directions as compared to non-viscous flow. In addition, a change in the location of the bubble center was also found due to viscosity (that may be implied from its initial creation location). The elliptic relation of the bubble geometry was found to be dependent on Reynolds number and not only the cavitation number as has typically been thought. Moreover, the slenderness parameter

of supercavitation bubble for a viscous flow showed dependency on Reynolds number together with the cavitation number with a similarity to Garbedian [34] relation and the asymptotic relation of Serebryakov [33] for non-viscous flows.

Author Contributions: This is an academic research. It was conducted in full collaboration and involvement of both authors, as is commonly done by a student (L.A.L.) and thesis Advisor (A.G.), with regards to conceptualization, evaluation, and presentation of the results. All authors have read and agreed to the published version of the manuscript.

Funding: This research was (partially) supported by PMRI—Peter Munk Research Institute, Technion.

Institutional Review Board Statement: Not applicable.

Informed Consent Statement: Not applicable.

Data Availability Statement: Not applicable.

Conflicts of Interest: The authors declare no conflict of interest.

References

1. Vanek, B.; Bokor, J.; Balas, G. High-speed supercavitation vehicle control. In Proceedings of the AIAA Guidance, Navigation, and Control Conference and Exhibit, Keystone, CO, USA, 21–24 August 2006; p. 6446. 2.
2. Ceccio, S.L. Friction Drag Reduction of External Flows with Bubble and Gas Injection. *Annu. Rev. Fluid Mech.* **2010**, *42*, 183–203. [CrossRef]
3. Logvinovich, G.V.; Serebryakov, V.V. On methods of calculating a shape of slender axisymmetric cavities. *Hydromechanics* **1975**, *32*, 47–54.
4. Serebryakov, V.V. *Asymptotic Solutions of Axisymmetric Problems of the Cavitation Flow under Slender Body Approximation, Hydrodynamics of High Speeds*; Chuvashian State University: Cheboksary, Russia, 1990; pp. 99–111.
5. Semenenko, V.N. Artificial Supercavitation. Physics and Calculation. In Proceeding of the RTO Lecture Series 005 on Supercavitating Flows, Brussels, Belgium, 7–9 April 2001.
6. Serebryakov, V.V. The models of the supercavitation prediction for high speed motion in water. In Proceedings of the International Scientific School: HSH-2002, Cheboksary, Russia, 16–23 June 2002.
7. Tulin, M.P. *Steady Two-Dimensional Cavity Flows about Slender Bodies*; Taylor Model Basin; David, W., Ed.; Department of the Navy, Research and Development Report 834: Washington DC, USA, 1953.
8. Gilbarg, D. *Free Stream Theory and Steady-State Cavitation*; Proc. Symposium On Naval Hydrodynamics: Washington, DC, USA, 1957; pp. 281–295.
9. Semenenko, V.N. Artificial Supercavitation, Physics and Calculation. In *Lecture Notes for the RTO AVT/VKI Special Course on Supercavitating Flows Von Karman Institute for Fluid Dynamics*; Defense Technical Information Center: Rhode Saint Genese, Belgium, 2001.
10. Vasin, A.D. Some Problems of Supersonic Cavitation Flows. Available online: <http://caltechconf.library.caltech.edu/82/> (accessed on 17 October 2021).
11. Vasin, A.D. Application of the Slender Body Theory to Investigation of the Developed Axially Symmetric Cavitation Flows in a Subsonic Stream of Compressible Fluid. *Izv. Vyssh. Uchebn. Zaved. Mat.* **2001**, *3*, 122–129. [CrossRef]
12. Vasin, A.D. *Supercavities in Compressible Fluid*; RTO EN-016; RTO AVT Lecture Series on “Supercavitating Flows”; von Kármán Institute VKI: Brussels, Belgium, 2001.
13. Vasin, A.D. Calculation of axisymmetric cavities downstream of a disk in a supersonic flow. *Fluid Dyn.* **1997**, *32*, 513–519.
14. Logvinovich, G.V. *Hydrodynamics of Free-Boundary Flows*; Naukova Dumka: Kyiv, Ukraine, 1969; p. 208.
15. Vasin, A.D. *The Principle of Independence of the Cavity Sections Expansion (Logvinovich’s Principle) as the Basis for Investigation on Cavitation Flows*; Project-Nerd: Arvada, CO, USA, 2001; Volume 2, pp. 161–162.
16. Serebryakov, V.V. Ring model for calculation of axisymmetric flows with developed cavitation. *J. Hydromech.* **1974**, *27*, 25–29.
17. Fu, H.; Lu, C.J.; Li, J. Numerical Research on Drag Reduction Characteristics of Supercavitating Body of Revolution. *J. Ship Mech.* **2004**, *8*, 1–7.
18. Yi, W.J. Research on drag characteristics of natural supercavitation profile for high speed bodies. *Ship Sci. Technol.* **2009**, *31*, 38–42.
19. Wu, T.Y.T.; Whitney, A.K.; Brennen, C. Cavity-flow wall effects and correction rules. *J. Fluid Mech.* **1971**, *49*, 223–256. [CrossRef]
20. Ahn, B.K.; Lee, T.K.; Kim, H.T.; Lee, C.S. Experimental investigation of supercavitating flows. *Int. J. Nav. Archit. Ocean. Eng.* **2012**, *4*, 123–131. [CrossRef]
21. Ahn, B.K.; Jeong, S.W.; Kim, J.H.; Shao, S.; Hong, J.; Arndt, R.E. An experimental investigation of artificial supercavitation generated by air injection behind disk-shaped cavitators. *Int. J. Nav. Archit. Ocean. Eng.* **2017**, *9*, 227–237. [CrossRef]
22. Karn, A.; Arndt, R.; Hong, J. An experimental investigation into supercavity closure mechanisms. *J. Fluid Mech.* **2016**, *789*, 259–284. [CrossRef]

23. Fridman, G.M.; Achkinadze, A.S. *Review of Theoretical Approaches to Nonlinear Supercavitating Flows*; Saint Petersburg State Marine Technical University, Ship Theory Department: St Petersburg, Russia, 2001.
24. Kirschner, I.I.; Chamberlin, R.; Arzoumanian, S.A. Simple approach to estimating three-dimensional supercavitating flow fields. In Proceedings of the 7th International Symposium on Cavitation CAV2009, Ann Arbor, MI, USA, 16–20 August 2009.
25. Arad Ludar, L.; Gany, A. Experimental Study of Supercavitation Bubble Development over Bodies in a Free-Surface Flow. *J. Mar. Sci. Eng.* **2022**, *10*, 1244. [[CrossRef](#)]
26. Arad Ludar, L.; Gany, A. Experimental study of supercavitation bubble development over bodies in a duct flow. *J. Mar. Sci. Eng.* **2020**, *8*, 28. [[CrossRef](#)]
27. Brennen, C.A. numerical solution of axisymmetric cavity flows. *J. Fluid Mech.* **1969**, *37*, 671–688. [[CrossRef](#)]
28. Kinnas, S.A. The prediction of unsteady sheet cavitation. In Proceedings of the 3rd International Symposium on Cavitation, Grenoble, France, 7–10 April 1998.
29. Scardovelli, R.; Zaleski, S. Direct numerical simulation of free-surface and interfacial flow. *Annu. Rev. Fluid Mech.* **1999**, *31*, 567–603. [[CrossRef](#)]
30. Shi, H.H.; Wen, J.S.; Zhu, B.B.; Chen, B. Numerical simulation of the effect of different object nose shapes on hydrodynamic process in water entry. Proceeding of the 10th International Symposium on Cavitation, CAV2018, Baltimore, MD, USA, 14–16 May 2018.
31. Franc, J.P.; Michel, J.M. *Fundamentals of Cavitation*; Kluwer Academic Publishers: Dordrecht, The Netherlands, 2004.
32. Kunz, R.F.; Lindau, J.W.; Billet, M.L.; Stinebring, D.R. *Multiphase CFD Modeling of Developed and Supercavitating Flows*; Pennsylvania State Univ., University Park, Applied Research Lab: University Park, PA, USA, 2001.
33. Serebryakov, V.V. The annular model for calculation of axisymmetric cavity flows. *Kiev. Russ.* **1972**, *27*, 25–29.
34. Garabedian, P.R. Calculation of axially symmetric cavities and jets. *Pac. J. Math.* **1956**, *6*, 611–684. [[CrossRef](#)]